



A new chaos and global competitive ranking-based symbiotic organisms search algorithm for solving reactive power dispatch problem with discrete and continuous control variable

Enes Yalçın¹ · Ertuğrul Çam² · Müslüm C. Taplamacıoğlu³

Received: 19 May 2018 / Accepted: 26 November 2019 / Published online: 4 December 2019
© Springer-Verlag GmbH Germany, part of Springer Nature 2019

Abstract

In this paper, optimal reactive power dispatch problem (ORPD) is solved by using a new chaos and global competitive ranking-based symbiotic organisms search algorithm (A-CSOS). SOS is an effective meta-heuristic algorithm, especially for optimization problems with continuous variable, with important features such as the absence of any user-defined algorithmic parameters and the easily applicable. However, some essential features of SOS such as trap into local optima and slow convergence problems need to be improved in order to find better solutions for more complex, nonlinear, multi-modal optimization problems such as ORPD. In this study, to solve ORPD and enhance the capability of the standard SOS even further, A-CSOS algorithm is developed. To test the performance of the developed algorithm in ORPD, the both SOS and the proposed A-CSOS are applied to the two different objective functions including power loss minimization and total voltage deviation minimization in IEEE 57-, 118-, 300-bus power systems. According to the results of ten different test cases, the proposed method gives better solutions up to 15.3% and 40.52% than the state-of-art algorithms and SOS, respectively. Moreover, the convergence performance of A-CSOS is considerably better than all tried algorithms. The effectiveness of A-CSOS for solving ORPD and other complex constrained optimization problems is proofed by this study.

Keywords Optimal reactive power dispatch · Symbiotic organisms search · Adaptive chaotic symbiotic organisms search · Power loss minimization · Voltage profile improvement

1 Introduction

With the increase in power demand and generation, simultaneously economic and safe operation of power systems has become a current and important issue. In order to operate the power systems in an economical way, it is necessary to

use the existing infrastructure and capacity in the most efficient and optimal way. Minimization of power loss (P_{loss}) is one of the priorities of the power system operators in terms of achieving both technical and economic benefit. Optimal distribution of reactive power generation in a power system by tuning the control variables to minimize specific objective function and satisfy the numerous constraints is known as optimal reactive power dispatch (ORPD). According to grid code, it is not enough to minimize only the considered objective function such as the minimization of P_{loss} or total voltage deviation (TVD), but also all equality and inequality constraints must be satisfied simultaneously. Therefore, ORPD is a complex, nonlinear and non-convex problem.

It is seen from the literature survey that researchers have used deterministic approaches such as linear programming [1], nonlinear programming [2], quadratic programming [3] and interior point [4] for solving ORPD in early years. By the reason of the nonlinearity, non-differential, multi-modal, non-convex characteristics of the ORPD, the majority of the deterministic methods may be very sensitive to

✉ Enes Yalçın
gaziyalcine@gmail.com

Ertuğrul Çam
ertugrul_cam@yahoo.com

Müslüm C. Taplamacıoğlu
taplam@gazi.edu.tr

¹ Inspection Board, Turkish Electricity Transmission Co., Ankara, Turkey

² Department of Electrical and Electronics Engineering, Kirikkale University, Kirikkale, Turkey

³ Department of Electrical and Electronics Engineering, Gazi University, Ankara, Turkey

the starting point and converge to a local optimum point [5]. Instead of these methods, population-based algorithms and their hybrid or improved/modified versions, such as genetic algorithm (GA) [6], differential evolution (DE) [7], biogeography-based optimization (BBO) [8], seeker optimization algorithm (SOA) [9], gravitational search algorithm (GSA) and its variants [10, 11], particle swarm optimization (PSO) with an aging leader and challengers (ALC-PSO) [12], hybrid PSO and imperialist competitive algorithm (ICA) (PSO-ICA) [13], hybrid modified ICA and invasive weed optimization (IWO) (MICA-IWO) [14], hybrid PSO and GSA (PSOGSA) [15], multi-objective chaotic improved PSO (MOCIPSO) [16], firefly algorithm (FA) [17], gray wolf optimization (GWO) [18], moth-flame optimization (MFO) [19], water cycle algorithm (WCA) and gaussian bare-bones WCA (NGBWCA) [20], chaotic parallel vector evaluated interactive honeybee mating optimization (CPVEIHBMO) [21], ant lion optimization (ALO) [22], modified ALO (MALO) [23], exchange market algorithm (EMA) [24], have been proposed for solving the ORPD. However, one of the disadvantages of some of the above-mentioned algorithms is that they have various algorithmic parameters, which influence the solution significantly and require to be identified carefully. The crossover and mutation probability values for GA, acceleration and inertia weight parameters for PSO, gravitational and α constants for GSA, differentiation (or mutation) and crossover constants for DE, reflection, expansion and contraction coefficients for FA are just a few examples. These parameters affect the convergence speed and balance between exploration and exploitation. Since the performance of these algorithms is closely associated with these parameters, it is important and necessary to adjust them to their ideal values [25].

In 2014, the Symbiotic Organisms Search algorithm (SOS) has introduced a population-based meta-heuristic algorithm that does not require any user-defined algorithmic parameters [26]. SOS algorithm's underlying logic is symbiotic interaction behavior of organisms to survive in the ecosystem. SOS has been tested for unconstrained and constrained benchmark functions and yields better results than well-known algorithms [26].

While setting the optimal value of these algorithmic parameters is sometimes a challenging process, they fulfill an important mission of balancing the global and local search capabilities of algorithms in search space. The absence of such an algorithmic parameter in the SOS algorithm makes it difficult to maintain the global and local search balance of the algorithm [25]. Unfortunately, SOS algorithm seems to be able to trap into local optima points and converge late, especially in solving highly nonlinear and non-convex problems with much boundary conditions. This is also the case for the ORPD problem as the number of bus and control parameters increases. Therefore, the mentioned

frailties of the SOS algorithm needs to be eliminated. For this reason, studies are being done to improve the SOS algorithm and applied to various optimization problems. The quasi-oppositional SOS algorithm is developed and applied to load frequency control by Guha et al. [27]. The modified SOS algorithm is introduced and implemented on economic dispatch problem with valve-point effects by Secui [28]. The adaptive SOS algorithm is created by updating the benefit factor terms in SOS throughout the iteration and tested on structural design optimization problems by Tejani et al. [29]. Saha et al. proposed chaotic SOS (CSOS) algorithm by replacing the parasitism phase that one of the phases of SOS with a chaotic local search for unconstrained benchmark test functions and siting and sizing problem of distributed generators in radial distribution system in [25]. Chaotic local search (CLS) was used in CSOS [25], but CLS was applied only to the best organism. Although the algorithm's local search capability is enhanced by this way, it limits global search capabilities. Therefore, CSOS, like the SOS algorithm, unable to get rid of local optima points in solving more complex and non-convex optimization problems.

It is a frequently used method to obtain new algorithms by hybridizing existing algorithms with other algorithms or by adding extra features. Due to the positive impact of algorithms on local and global searching performance and easy implementation, chaos maps are an often-preferred healing method by researchers. In many heuristic algorithms, the "rand" operator is defined to increase the randomness of the solution candidates and the search capability in the solution space. The logistic map, one of the variance of chaos, known for their ergodicity, randomness and non-repeatability, have been found to improve algorithms search capability and convergence speed compared to rand operators. Along with the modification in the algorithm stages, it is important to improve the constraint handling mechanisms integrated with the algorithms. The most common classical method for constraint handling is the static penalty function (SPF) method, which involves penalty coefficients that must be defined by the user. The main problem with SPF method is that it requires many trial and error process to find the ideal value of the penalty coefficients. As a solution to this situation, the researchers define higher values than necessary for the penalty coefficients, but this causes the algorithms to be fell into local optima points. On the other hand, global competitive ranking (GCR), developed by Runarsson and Yao [30], quickly finds the nearest candidate solution to the global optimum point by making a balanced search in both the feasible and the infeasible region. By using algorithms such as SOS, CSOS or the other algorithms using SPF method it is very difficult and time consuming to find both minimum and feasible solutions to more complex and more constrained optimization problems like ORPD. The GCR provides substantial improvements in algorithmic speed by finding the feasible solution very quickly

without requiring any trial and error process. It also appears to improve the standard deviation values encountered in mentioned algorithms. inspired by these ideas, a new A-CSOS algorithm is developed by merging the logistic map and GCR constraint handling mechanism with SOS to eliminate the weakness of the SOS as mentioned earlier and enhance the exploration and exploitation skills of the SOS even further.

The main contributions of this paper are: developing a new A-CSOS algorithm, hybridizing the logistic map and global competitive ranking with SOS, eliminating the drawbacks in more complex and con-convex problems of the SOS such as being trapped into local optima and premature convergence, implementing the proposed A-CSOS and SOS on the ORPD problem. In order to analyze the performance of the A-CSOS and SOS, both algorithm are applied to the ORPD problem in IEEE 57-, 118-, 300-bus standard test systems. Since both P_{loss} and TVD minimization are studied as objective functions for each power systems, and some of control variables are considered the mix of discrete and continuous or fully continuous, the results of the proposed algorithm are evaluated in 10 different cases under six different scenarios in this study. Moreover, the proposed algorithm is not only compared with the SOS but also compared with other state-of-art algorithms. It is clear that the proposed A-CSOS yields up to 15.3% and 44.1% better results than many of the latest studies in literature and SOS. Therefore, A-CSOS algorithm is a promising method for ORPD and other constrained optimization problems.

The rest of this paper is organized as follows. ORPD problem is explained in Sect. 2. Description of the A-CSOS algorithm is given in Sect. 3. Implementation steps of A-CSOS for ORPD problem is described in Sect. 4. The studied scenarios and obtained results are presented in Sect. 5, conclusions are given in Sect. 6.

2 The ORPD problem formulation

Since ORPD is a nonlinear, non-convex and constrained optimization problem composed of a specific objective function to be optimized while satisfying numerous constraints, it is necessary to express mathematically each objective functions and constraints. In this work, two different objective functions including P_{loss} and TVD minimization are concerned separately for ORPD problem. Mathematical explanation of these objective functions and constraints are explained in the next sub-sections.

2.1 Objective functions

2.1.1 Minimization of P_{loss}

ORPD solution is mainly to minimize P_{loss} in the existing branches while fulfilling all constraints. Minimization of active power loss can be mathematically stated by Eq. (1).

$$f_1(x, u) = \sum_{l=1}^{N_L} \left[G_l \left(V_i^2 + V_j^2 - 2V_i V_j \cos \delta_{ij} \right) \right] \tag{1}$$

where N_L is the number of branch, G_l is the conductance of branch- l connecting buses i and j ; V_i and V_j are voltage magnitudes at buses i and j , respectively; and δ_{ij} is the phase difference between buses i and j , respectively.

2.1.2 Minimization of TVD

The second objective function used in this study is TVD that aims to minimize absolute deviations of all the present load bus voltages from the referenced magnitude. Thus, voltage profile can be enhanced by this way. The mathematical expression of TVD minimization problem is described as follows:

$$f_2(x, u) = \sum_{k=1}^{N_{PQ}} \left| V_k - V_k^{ref} \right| \text{ (where } V_k^{ref} = 1 \text{ p.u.)} \tag{2}$$

where N_{PQ} is the number of PQ bus, V_k is the voltage of PQ bus- k , V_k^{ref} is desired voltage at bus- k .

Each objective function is related to the state/dependent and control/independent variables denoted by x and u , respectively. The dependent variable vector is composed of the voltages of PQ-bus (V_L), Mvar output of generators (Q_G) and MVA loading of branches (S_L), while independent variable vector is composed of the voltages of PV bus (V_G), the tap ratios of transformers (T_N) and Mvar output of shunt compensators (Q_C).

$$x = \left[V_{L_1}, \dots, V_{L_{N_{PQ}}}, Q_{G_1}, \dots, Q_{G_{N_{PV}}}, S_{L_1}, \dots, S_{L_{N_L}} \right] \tag{3}$$

$$u = \left[V_{G_1}, \dots, V_{G_{N_{PV}}}, T_1, \dots, T_{N_T}, Q_{C_1}, \dots, Q_{C_{N_C}} \right] \tag{4}$$

where N_{PV} is the number of PV bus, N_T is the number of transformers, and N_C is the number of shunt compensators.

2.2 Constraints

2.2.1 Equality constraints

The equality constraints “ $g(x, u)$ ” for ORPD problem are described using power balance formulas expressed by Eqs. (5)–(6) [11].

$$P_{G_i} - P_{L_i} = V_i \sum_{j \in N_i} V_j \left[G_{ij} \cos \theta_{ij} + B_{ij} \sin \theta_{ij} \right] \tag{5}$$

$$Q_{G_i} - Q_{L_i} = V_i \sum_{j \in N_i} V_j \left[G_{ij} \sin \theta_{ij} - B_{ij} \cos \theta_{ij} \right] \tag{6}$$

where N_i is the number of buses connected to bus- i , P_{Gi} and Q_{Gi} are the MW and Mvar generation, respectively; P_{Li} and Q_{Li} are the MW and Mvar demand; G_{ij} and B_{ij} are the conductance and susceptance, respectively.

2.2.2 Inequality constraints

The lower and upper limit values of the essential parameters for the grid are defined in the grid codes so that the grid can be safely operated by transmission system operators (TSOs) and distribution system operators (DSOs). In addition, the existing equipment in the grid has its own operating limits. The limits in this context including the limits of PV and PQ bus voltages, Mvar output of generators and shunt VAR compensators, transformers' taps, transmission line loading capacities constitute the inequality constraints denoted by $h(x, u)$ and expressed below, respectively.

$$V_{Gi}^{\min} \leq V_{Gi} \leq V_{Gi}^{\max}, \quad i \in N_G \quad (7)$$

$$V_{Li}^{\min} \leq V_{Li} \leq V_{Li}^{\max}, \quad i \in N_{PQ} \quad (8)$$

$$Q_{Gi}^{\min} \leq Q_{Gi} \leq Q_{Gi}^{\max}, \quad i \in N_G \quad (9)$$

$$Q_{Ci}^{\min} \leq Q_{Ci} \leq Q_{Ci}^{\max}, \quad i \in N_C \quad (10)$$

$$T_i^{\min} \leq T_i \leq T_i^{\max}, \quad i \in N_T \quad (11)$$

$$|S_{Li}| \leq S_{Li}^{\max}, \quad i \in N_L \quad (12)$$

The superscripts min and max used in Eqs. (7–12) mean the corresponding lower and upper limits, respectively.

3 The proposed technique

3.1 Symbiotic organisms search algorithm

The SOS algorithm is one of the new meta-heuristic population-based algorithm introduced in 2014 [26]. This algorithm simulates symbiotic reciprocations between different organisms living in an ecosystem.

The fundamental relations between different species in universe are mutualism, commensalism, and parasitism. These interactions are modeled in SOS by their mathematical expressions given in the following sub-headings.

3.1.1 Mutualism

The mutualism phase simulates to the reciprocal action between two different organisms where both of them get

benefited from this relation. X_{i_org} and X_{j_org} , which enter into mutualist relation and denote to i th and j th organism in the ecosystem, may benefit from each other at equal or different rates. Two new, but temporary organisms, X_{i_temp} and X_{j_temp} are produced after performing mutualism relation. It replaces the better one by comparing the newly produced organisms with originals. The mutualism process mathematically can be described by Eqs. (13) and (14) [26].

$$X_{i_temp} = X_{i_org} + rand(0, 1)(X_{best} - mVector \times bF_1) \quad (13)$$

$$X_{j_temp} = X_{j_org} + rand(0, 1)(X_{best} - mVector \times bF_2) \quad (14)$$

In above equations, X_{best} is an organism with the highest degree of adaption and gives the best solution so far in the ecosystem; $rand(0, 1)$ is a random number between 0 and 1; $mVector$, bF_1 , and bF_2 are calculated using Eqs. (15)–(17).

$$mVector = \frac{X_{i_org} + X_{j_org}}{2} \quad (15)$$

$$bF_1 = round(1 + rand(0, 1)) \quad (16)$$

$$bF_2 = round(1 + rand(0, 1)) \quad (17)$$

where bF_1 and bF_2 are the beneficial factors which show the rate of profit from each other. As can be understood from Eqs. 16 and 17, bF_1 and bF_2 can take a value of four possible combinations. If bF_1 and bF_2 take equal values, it means that both organisms benefit equally in mutualist relation to each other, otherwise an organism will benefit more from this relation than the other.

3.1.2 Commensalism

Unlike the mutualism phase, only one organism gets to benefit from this dependency between two different organisms. The other is not affected significantly. Similarly, X_{i_org} is an organism that corresponds to organism- i in the ecosystem and X_{j_org} is an arbitrary selected organism that interacts with X_{i_org} . In this phase, X_{i_org} attempts to acquire benefit from X_{j_org} , while X_{j_org} is not affected negatively or positively. The new temporary obtained organism after performing commensalism process X_{i_temp} is formulated by Eq. (18).

$$X_{i_temp} = X_{i_org} + rand(-1, 1)(X_{best} - X_{j_org}) \quad (18)$$

3.1.3 Parasitism

In the parasitism phase, one organism takes advantage from this relationship while the other is damaged. X_{i_org} is an organism that represents the parasite vector which is the

duplicating form of X_{i_org} and X_{j_org} is a randomly selected organism that hosting the parasite vector and interacting with X_{i_org} . In this phase, X_{j_org} is modified by interacting with parasite vector. The infected and parasite vector's fitness value are calculated separately. The infected vector must have a better fitness value than the parasite vector to maintain its position. Otherwise, the parasite vector kills and replaces the infected vector.

3.2 Adaptive chaotic symbiotic organisms search algorithm

The most important feature that makes the SOS algorithm attractive is that not necessitate any user-defined algorithmic parameters. This requirement affects negatively both the performance of the other algorithms and causes a lot of time loss. However, the SOS algorithm has some adverse properties need to be solved. The most important of these is that it is easily lodged in local optimum points, especially in the solution of complex non-convex problems.

Various modifications have been made in the literature to overcome these deficiencies in the SOS algorithm. In this context, the chaotic local search feature has been added to the SOS in CSOS [25], but limited local search capability has been developed since chaos is only applied to the best organism and the parasitism phase is removed. In addition, this can lead to an unbalanced search in the global and local search space and trap into local optima because it increases the orientation toward the best organism. It is important to develop both the local and global exploring capabilities of the SOS so that it can be overcome by all sorts of challenging problems. In addition, some characteristics such as the convergence speed of the SOS algorithm can still be improved.

Another important issue is that for constrained optimization problems, an integrated constraint handling strategy that works in an efficient and compatible manner with the algorithm is required. Constraint handling mechanisms support the performance of algorithms. If this is ignored, the algorithm is inherently capable, but cannot be exploited enough without the algorithm due to the constraint handling methodology.

In order to remove the problems mentioned above, two important contributions have been integrated to the SOS algorithm: the logistic map that is one of the chaos functions, and the global competitive ranking that is one of the adaptive penalty strategies. Finally, a new algorithm named A-CSOS is obtained. The changes made on the SOS algorithm can be categorized as chaos adaptation to mutualism phase, chaos adaptation to commensalism phase, and Global Competitive Ranking (GCR) constraint handling integration. It should be noted that in this study chaos is applied not only to the best organism but also to all the organisms in the ecosystem in

order to be able to make a more effective search in the local and global search space. The details of modifications are explained in the following sub-headings.

3.2.1 Increasing randomness of mutualism with logistic map

Chaos maps are known to significantly improve the exploration and exploitation capabilities of the algorithms. In some of the studies in which chaos is integrated, chaos is only used during the generation of initial population phase, while in others it is adapted to some stages of the algorithm. Although various chaos functions are proposed depending on the problem in the studies, logistic map is the most known of these.

The *rand* expression in Eqs. (13)–(14) affects the organism's range of motion and local search abilities. Therefore, logistic map is implemented on random statements of X_{i_temp} and X_{j_temp} formulas in mutualism phase and the equations of mutualism phase are modified as follows:

$$X_{i_temp} = X_{i_org} + c_i^t (X_{best} - mVector \times bF_1) \quad (19)$$

$$X_{j_temp} = X_{j_org} + c_j^t (X_{best} - mVector \times bF_2) \quad (20)$$

$$c_{i,k}^t = \mu \times c_{i,k-1}^t \times (1 - c_{i,k-1}^t) \quad \text{where } 0 < \mu \leq 4 \quad (21)$$

where $c_{i,k}^t$ denotes the k th chaotic variable of i th organism in the t th iteration. μ is called control parameter and $c_{i,k}^t \in (0, 1)$. The value of μ affects the behavior of the steady-state solution of this map. For $\mu \in (0, 1)$, $c_{i,k}^t$ tends to zero; for $\mu \in [1, 3)$, a fixed point; for $\mu \in [3, 3.57)$, periodic; and finally for $\mu \in [3.57, 4)$, chaotic. Therefore, the output $c_{i,k}^t$ is aperiodic, non-convergent and very sensitive to the initial value of $c_{i,0}^t$, which is not equal to $\{0, 0.25, 0.5, 0.75, 1\}$. Although μ can also set close to 4, $\mu = 4$ assures that the equation is chaotic [31].

3.2.2 Increasing randomness of commensalism with logistic map

The *rand*(-1, 1) expression in Eq. (18) affects the exploration and exploitation performance of the SOS algorithm. Therefore, logistic map is implemented on *rand*(-1, 1) statement of X_{i_temp} formula in commensalism phase. The new commensalism phase equation after the modification can be rewritten as follow:

$$X_{i_temp} = X_{i_org} + (2c_i^t - 1) \times (X_{best} - X_{j_org}) \quad (22)$$

3.2.3 Global competitive ranking-based constraint handling methodology

To satisfy equality and inequality constraints, a constrained problem converts into an unconstrained problem by adding a penalty value to the objective function. This method is known as static penalty function (SPF). The general formula of SPF integrated with ORPD can be expressed as follows:

$$F(X_i) = f_n(X_i) + \tau_v \sum_{i=1}^{N_{PQ}} (V_{Li} - V_{Li}^{\text{lim}})^2 + \tau_q \sum_{i=1}^{N_G} (Q_{Gi} - Q_{Gi}^{\text{lim}})^2 \quad (23)$$

In Eq. (23), f_n is described as the objective function either P_{loss} or TVD value. τ_v and τ_q are expressed as static penalty factors for voltage and reactive power constraints, respectively; V_{Li}^{lim} and Q_{Gi}^{lim} are the limit values of PQ bus voltage and generator reactive power output, respectively.

The main handicap of the SPF method is that it requires a time-consuming trial-and-error process to adjust the penalty coefficients affecting solution accuracy. This situation also overshadows the algorithmic parameterless nature of the SOS algorithm. Therefore, instead of the SPF method, GCR mechanism that more accurately and quickly converges to the global optimum point by correctly interpreting the information it receives from the SOS algorithm is proposed.

GCR is a sorting-based adaptive penalty method developed by Runarsson and Yao [30]. GCR is an advanced version of stochastic ranking (SR) [32]. Unlike SR, a solution candidate is sorted by analogizing it with not the only adjacent neighborhood but also all other members of the population. Another difference between SR and GCR is that fitness evolution is made according to both objective function and constraint violation at the rate of P_f in GCR. The fitness level of each individual in the GCR method can be evaluated as follows [30]:

$$F(X_i) = P_f \frac{\text{rank}(f(X_i)) - 1}{N_{\text{pop}} - 1} + (1 - P_f) \frac{\text{rank}\left(\sum_{j=1}^m v_j(X_i)\right) - 1}{N_{\text{pop}} - 1} \quad (24)$$

$$v_j(X_i) = \max\{0, g_j(X_i)\} \quad (25)$$

In Eq. (24), $F(X_i)$ is the actual fitness value of organism- i , $\text{rank}(f(X_i))$ represents the actual rank of i th organism in the population considering objective function value; $\text{rank}\left(\sum_{j=1}^m v_j(X_i)\right)$ represents the actual rank of i th organism in the population considering the sum of its constraint violations, N_{pop} is the number of individuals, P_f symbolize the probability that fitness is calculated based on the rank of objective function. It is recommended that the value of P_f be between 0 and 0.5 to find both a feasible and a minimum solution.

4 Implementation of the A-CSOS algorithm for ORPD problem

Creating the ecosystem is the first phase of the A-CSOS algorithm. An ecosystem comprises a number of organisms. Each organism represents a candidate solution in search space. The ecosystem, in other words control variable vector including generator set voltages, reactive power outputs of shunt VAR compensators and tap settings of transformers is created randomly considering their limits. Moreover, basic parameters like the number of organisms, maximum number of iteration, maximum and minimum limits of related variables are also defined in this phase. The bus, generator and branch data of each test system are prepared.

Secondly, each organism is exposed to Newton–Raphson power flow using the Matpower and then objective function and the sum of constraint violation values are calculated from the obtained results. In accordance with GCR method, organisms in the ecosystem are separately ranked according to their objective function and sum of the constraint violation value. The fitness function value of each organism is calculated by using Eq. (24).

Thirdly, mutualism, commensalism and parasitism relationship are established between X_i and randomly selected organism X_j until the predefined maximum iteration is achieved. Nevertheless, unlike the mathematical expressions of mutualism and commensalism phases of conventional SOS, Eqs. (19–22) are used that is highlighted in Fig. 1.

5 Results and discussion

A-CSOS and SOS algorithms are implemented on ORPD problem for IEEE 57-, 118- and 300-bus standard power systems. Two different objective functions are studied including P_{loss} and TVD minimization for each test case for understanding performance of the A-CSOS. Algorithms are implemented using the MATLAB R2013a and applied on a 2.60 GHz Intel Core i5 with 4 GB RAM notebook. Due to a fair evolution of the simulation results, Matpower software [33] is selected for power flow analysis. For each case, above-mentioned boundary conditions are also checked in Matpower. The maximum number of iteration is 100 for IEEE 57-, 118-bus simulation analysis, and 200 for IEEE 300-bus simulation analysis. The numbers of organism in the simulations are taken as 30 for IEEE 57-bus, 50 for IEEE 118-bus, 75 for IEEE 300-bus power system. The algorithm is tested with 100 runs of each test case. The best, mean and standard deviations of each objective functions after 100 runs are given in the related sub-sections.

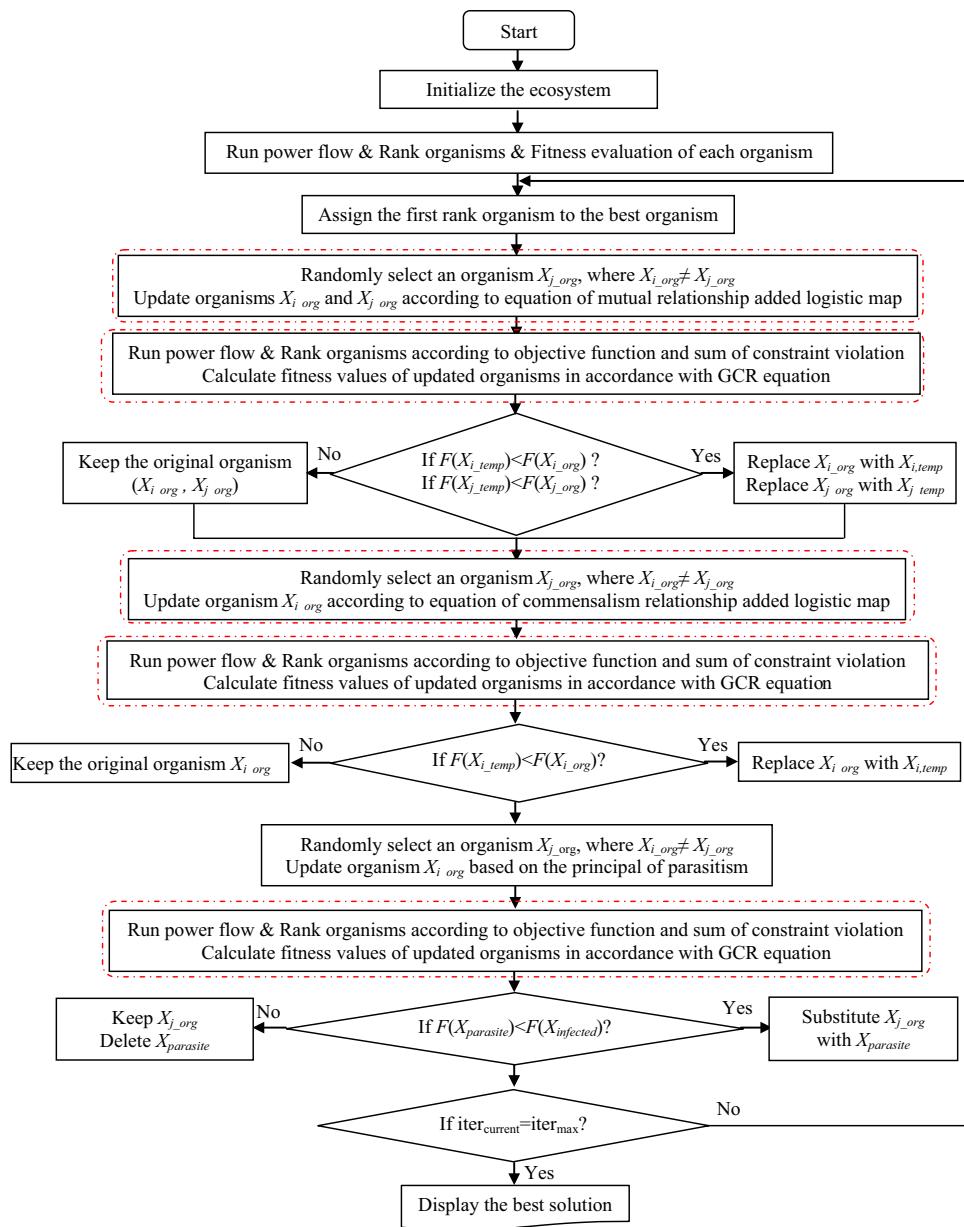


Fig. 1 Flowchart of A-CSOS algorithm-based reactive power dispatch

However, it is useful to first investigate the effect on the results of the value of benefit factors, since these values are taken into account in the other results given in the following headings. The beneficial factors can be taken two different values, 1 or 2. Beneficial factor is critical because it determines the direction of motion of organisms and express the benefit degree of organisms to each other. A deep analysis of the best results for all scenarios revealed that bF_1 and bF_2 parameters are equal to 1. The statistical results of analyses carried out for IEEE-57 bus system are presented in Table 1.

As can be seen in Table 1, the worst solution for all cases has been obtained when both bF_1 and bF_2 are equal to 2. On the other hand, the algorithm when both bF_1 and bF_2 are equal to 1 is much better in terms of best, mean and standard deviation values for all test scenarios. The results confirm that adjusting the benefit factors of the SOS strengthened the ability of the SOS and the algorithm become more stable and promising. Therefore, both bF_1 and bF_2 have been taken as 1 for the results given in the paper.

Table 1 The effect of bF_1 and bF_2 on the simulation results

Objective		bF_1 and bF_2		
Function		1	1 or 2	2
<i>P_{loss} minimization</i>				
Scenario 1.1	Best	23.81930	23.82537	24.96960
	Mean	23.91820	24.23793	28.59416
	Std.	0.344870	0.569286	1.893115
Scenario 1.2	Best	23.82610	23.84012	24.80120
	Mean	24.05490	24.74526	29.05011
	Std.	0.452563	0.943265	1.572828
<i>TVD minimization</i>				
Scenario 2.1	Best	0.661740	0.666830	0.862580
	Mean	0.685835	0.703160	0.703160
	Std.	0.018488	0.040748	0.040748
Scenario 2.2	Best	0.668900	0.699484	0.905440
	Mean	0.705900	0.715332	1.079061
	Std.	0.031790	0.038233	0.076371

5.1 Test System 1: IEEE 57-bus power system

The IEEE 57-bus power system has 25 control variables including seven PV bus voltages, fifteen transformers' tap ratios and three shunt VAR compensators. Test system data are adapted from [28]. The permissible voltage limits at load and generator buses are 0.95–1.05 p.u. and 0.95–1.1 p.u., respectively. The permissible limits of transformer tap ratios are 0.9–1.1 p.u. The permissible Mvar limits of shunt capacitor linked to bus-18, -25 and -53, respectively are set to 0–10 Mvar, 0–5.9 Mvar, and 0–6.3 Mvar. The proposed algorithm and studied SOS algorithm are applied to IEEE 57-bus test system for minimization of P_{loss} as Scenario 1 and minimization of TVD as Scenario 2. Transformer taps and VAR compensators are considered continuous in Scenario 1.1 and 2.1, and discrete with the 0.01 p.u. stepwise in Scenario 1.2 and 2.2.

Comparison of the best results of proposed A-CSOS with SOS algorithm and the best results of other state-of-the-art optimization techniques such as self-adaptive differential evolution (L-SaDE) [9], SOA [9], comprehensive learning particle swarm optimizer (CLPSO) [9], ABC [23], FA [23], BAT [23], ALO [23], MALO [23], MFO [19], hybrid PSO-ICA [13], modified ICA and IWO (MICA-IWO) [14], MOCIPSO [16], OGSA [11] for Scenario 1 and 2 are given in Tables 2 and 3, respectively.

Table 4 demonstrates the best solutions for each scenario and optimal values of variables. After applying the A-CSOS algorithm to IEEE 57-bus test system, P_{loss} is reduced to a minimum value of 23.8193 MW (Scenario 1.1) and 23.8284 MW (Scenario 1.2) from the initial case P_{loss} of 27.8638 MW. It is clear that approximately the same and the best results are obtained via A-CSOS and SOS algorithms

for each scenario. The result of A-CSOS is 0.4336 MW (1.79%) better than the MALO [19] that is the best result of above-mentioned algorithms considering continuous variables.

According to the result of Scenario 1.2, A-CSOS yields 0.0716 MW better than MALO [23], which is the best result of given algorithms. As can be seen in Figs. 2 and 3, all dependent variables are within permissible limits after Scenario 1 and Scenario 2 optimizations, respectively.

While the results obtained from A-CSOS and SOS algorithms in Scenario 1 are close to each other, there is an important difference between the results of the two algorithms obtained under Scenario 2. According to Scenario 2.1 results shown in Table 3, the proposed algorithm is 4.44% better than SOS and 5.22% better than OGSA [11] algorithm with the lowest value among the algorithms shown in Table 3. In the Scenario 2.2 analysis, the A-CSOS algorithm yielded a 4.18% better result than the SOS, and 15.32% better than the MALO [23], which regarded the control variables as discrete.

To illustrate the convergence profile of A-CSOS and SOS algorithms, P_{loss} and TVD value changes over 100 iterations are demonstrated in Figs. 4 and 5, respectively.

There is a great difference between the convergence speed of A-CSOS and SOS. As Fig. 4 shows, A-CSOS converges to the minimum optimal solution about the fifteenth iteration while SOS needs twenty-five more iterations to converge.

Table 2 Comparison of the results for Scenario 1

Algorithms	Min P_{loss} , MW	Mean P_{loss} , MW	Std.
PSO [13]	27.5543	NR ^b	NR ^b
MOCIPSO ^a [16]	27.0750	NR ^b	NR ^b
ICA [13]	26.9996	NR ^b	NR ^b
CLPSO ^a [9]	25.7968	27.3334	1.9252E–02
PSO-ICA [13]	25.5856	NR ^b	NR ^b
ALO ^a [23]	25.1000	25.3338	4.4E–01
L-SaDE ^a [9]	24.6712	26.0983	1.3426E–02
SOA ^a [9]	24.6248	25.7410	1.1918E–02
IWO ^a [14]	24.5939	26.5769	1.7332E–02
ABC ^a [23]	24.3000	NR ^b	NR ^b
MICA-IWO ^a [14]	24.2568	24.2756	2.3361E–04
MFO [19]	24.2529	24.7702	NR ^b
BAT ^a [23]	24.1000	NR ^b	NR ^b
FA ^a [23]	24.1000	NR ^b	NR ^b
MALO ^a [23]	23.9000	23.9519	4.58E–02
SOS ^a	23.8670	27.1009	1.7193
A-CSOS ^a	23.8284	24.7216	9.3634E–01
SOS	23.8566	26.4900	1.5933
A-CSOS	23.8193	24.2295	6.1438E–01

^aDiscrete variable is considered in this result

^bNot reported

Table 3 Comparison of the results for Scenario 2

Algorithms	Min TVD, pu	Mean TVD, pu	Std.
BAT ^a [23]	0.8800	NR ^b	NR ^b
ABC ^a [23]	0.8400	NR ^b	NR ^b
FA ^a [23]	0.8200	NR ^b	NR ^b
PSO [13]	0.8007	NR ^b	NR ^b
ALO ^a [23]	0.8000	0.850817	0.03245
ICA [13]	0.7952	NR ^b	NR ^b
MALO ^a [23]	0.7900	0.8021	0.00636
PSO–ICA [13]	0.7130	NR ^b	NR ^b
OGSA [11]	0.6982	NR ^b	NR ^b
SOS ^a	0.69821	0.93090	0.138573
A-CSOS ^a	0.66899	0.70502	0.023933
SOS	0.69252	0.90414	0.142248
A-CSOS	0.66174	0.69816	0.031045

^aDiscrete variable is considered in this result

It is observed in Fig. 5 that A-CSOS converges faster as compared to SOS and the results are very promising in all scenarios. The obtained best solution is achieved about the twentieth iteration. It is also noted that logistic map has been very effective to generate organism from the first iteration. Hence, it can be concluded that both the chaos and adaptive penalty approaches are a significant positive contribution to convergence speed.

5.2 Test System 2: IEEE 118-bus power system

Considering that today’s power systems are more complex, it is important to proof the performance of the A-CSOS algorithm in larger power systems. For this reason, P_{loss} and TVD minimization for IEEE 118-bus power system are studied as Scenario 3 and Scenario 4, respectively. As in analyses on Test System 1, the mentioned variables are considered as discrete in Scenarios 3.2 and 4.2. Seventy-seven control parameters have to be adjusted for the solution of the ORPD problem in IEEE 118-bus test system consisting of

Table 4 Optimal value of control variables for best result of P_{loss} and TVD optimization on Test System 1

Variable	Scenario 1.1		Scenario 1.2		Variable	Scenario 2.1		Scenario 2.2	
	A-CSOS	SOS	A-CSOS	SOS		A-CSOS	SOS	A-CSOS	SOS
V_{G1} (p.u.)	1.07720	1.0804	1.0773	1.0760	V_{G1} (p.u.)	1.00330	1.0030	1.00360	0.9884
V_{G2} (p.u.)	1.07350	1.0752	1.0742	1.0726	V_{G2} (p.u.)	0.98738	1.0133	1.01050	0.9744
V_{G3} (p.u.)	1.05530	1.0529	1.0573	1.0557	V_{G3} (p.u.)	1.01780	1.0147	1.02030	1.0139
V_{G6} (p.u.)	1.04700	1.0444	1.0479	1.0517	V_{G6} (p.u.)	1.00120	1.0016	0.99992	1.0072
V_{G8} (p.u.)	1.06510	1.0609	1.0661	1.0664	V_{G8} (p.u.)	1.02390	1.0299	1.02480	1.0247
V_{G9} (p.u.)	1.04510	1.0400	1.0464	1.0462	V_{G9} (p.u.)	1.01810	1.0221	1.01850	1.0216
V_{G12} (p.u.)	1.03670	1.0311	1.0364	1.0387	V_{G12} (p.u.)	1.03190	1.0327	1.03120	1.0483
T_{4-18} (p.u.)	0.95340	1.0613	0.9600	0.9500	T_{4-18} (p.u.)	1.00210	0.9883	0.91000	1.0700
T_{4-18} (p.u.)	1.02330	0.9471	0.9900	1.0000	T_{4-18} (p.u.)	0.97362	0.9851	1.05000	0.9100
T_{21-20} (p.u.)	1.01150	1.0179	1.0100	1.0100	T_{21-20} (p.u.)	0.97264	0.9765	0.98000	0.9800
T_{24-26} (p.u.)	1.00910	1.0071	1.0100	1.0200	T_{24-26} (p.u.)	1.05790	1.0687	1.06000	1.0700
T_{7-29} (p.u.)	0.98933	0.9863	0.9900	0.9900	T_{7-29} (p.u.)	0.95110	0.9439	0.95000	0.9500
T_{34-32} (p.u.)	0.97089	0.9706	0.9600	0.9700	T_{34-32} (p.u.)	0.90722	0.9132	0.91000	0.9100
T_{11-41} (p.u.)	0.90635	0.9043	0.9100	0.9100	T_{11-41} (p.u.)	0.90000	0.9000	0.90000	0.9000
T_{15-45} (p.u.)	0.99006	0.9886	0.9900	0.9900	T_{15-45} (p.u.)	0.94288	0.9491	0.95000	0.9500
T_{14-46} (p.u.)	0.96721	0.9633	0.9700	0.9700	T_{14-46} (p.u.)	0.97986	0.9882	0.98000	0.9900
T_{10-51} (p.u.)	0.97567	0.9696	0.9800	0.9800	T_{10-51} (p.u.)	1.00940	1.0199	1.01000	1.0200
T_{13-49} (p.u.)	0.93572	0.9295	0.9400	0.9400	T_{13-49} (p.u.)	0.90000	0.9000	0.90000	0.9000
T_{11-43} (p.u.)	0.97677	0.9725	0.9800	0.9800	T_{11-43} (p.u.)	0.95827	0.9490	0.96000	0.9600
T_{40-56} (p.u.)	1.00130	0.9979	1.0000	1.0000	T_{40-56} (p.u.)	1.02790	0.9762	1.03000	1.0300
T_{39-57} (p.u.)	0.96479	0.9637	0.9600	0.9600	T_{39-57} (p.u.)	0.90008	0.9946	0.90000	0.9100
T_{9-55} (p.u.)	0.98756	0.9824	0.9900	0.9900	T_{9-55} (p.u.)	0.98975	1.0142	0.99000	1.0000
Q_{C18} (MVar)	8.20720	9.9999	1.8000	2.0100	Q_{C18} (Mvar)	0.21433	3.9849	4.22000	1.3300
Q_{C25} (MVar)	5.89160	5.8994	5.9000	5.7400	Q_{C25} (Mvar)	5.90000	5.9000	5.90000	5.8800
Q_{C53} (MVar)	6.27600	6.2990	6.3000	5.8300	Q_{C53} (Mvar)	6.29790	5.6544	6.30000	6.2900
P_{loss} (MW)	23.8193	23.8566	23.8284	23.8670	TVD (p.u.)	0.66174	0.6925	0.66899	0.6982
CPU time (s)	263.1987	257.1323	265.5406	264.1323	CPU time (s)	286.2552	280.0591	289.6801	285.3849

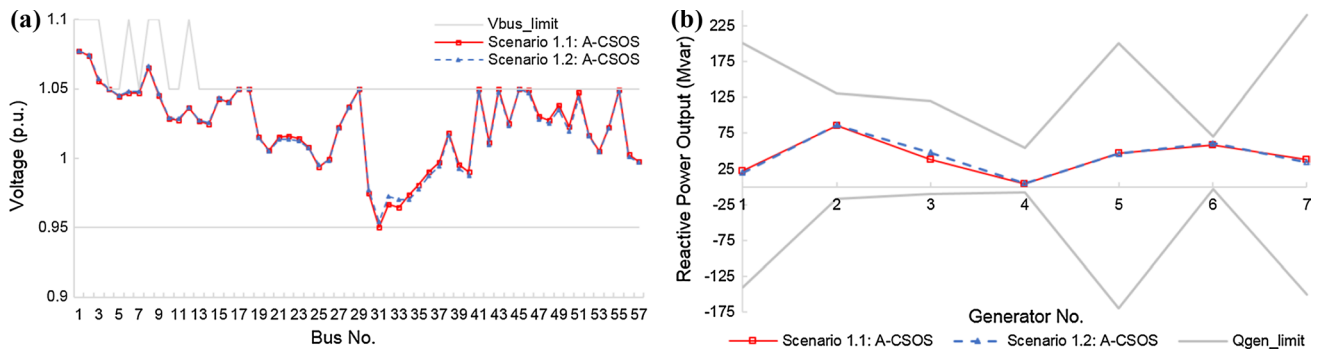


Fig. 2 Dependent variable profiles after Scenario 1 (P_{loss} optimization). **a** Bus voltage profiles. **b** Mvar output of generators

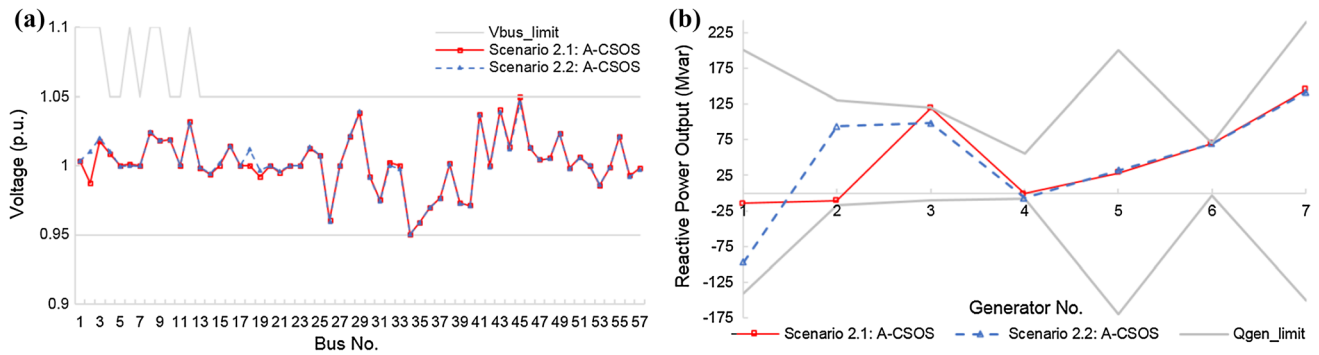


Fig. 3 Dependent variable profiles after Scenario 2 (TVD optimization). **a** Bus voltage profiles. **b** Mvar output of generators

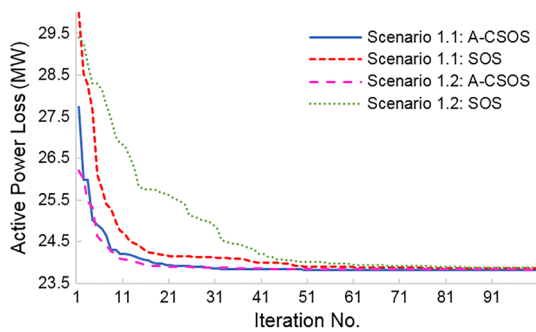


Fig. 4 The convergence profiles for Scenario 1

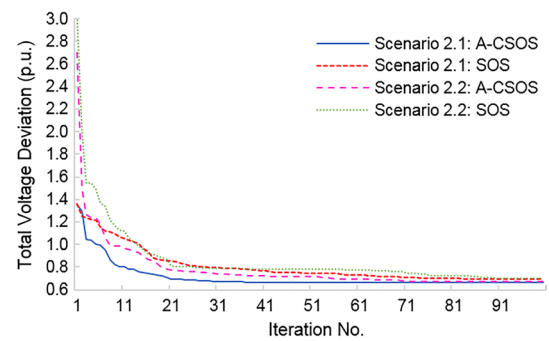


Fig. 5 The convergence profiles for Scenario 2

fifty-four generators, nine transformers, and fourteen shunt VAR compensators. The bus, generator, and line data are adapted from [33]. The lower and upper permissible voltages at PQ and PV buses are 0.94 and 1.06 p.u., respectively. The permissible tap ratio limits set to 0.9–1.1 p.u.

The comparison of the best result of A-CSOS with SOS and the most recent ORPD studies for Scenario 3 are given in Table 5. The optimal control variable settings for the best result of Scenario 3 are demonstrated in Table 6.

It is clear from Tables 5 and 6 that, in contrast to Scenario 1, where the number of bus is increased and the

power system is more complex, the superiority of the proposed algorithm over the SOS is more obvious.

In addition, as the number of buses increases, it becomes difficult to find a feasible and minimum solution for the SOS. The active power loss is reduced to 118.4089 MW and 119.4842 MW from the initial case P_{loss} of 132.8629 MW via A-CSOS for Scenario 3.1 and 3.2, respectively. Moreover, A-CSOS algorithm is 4.45% and 1.86% better than standard SOS and GWO [18], which is the best result of declared state-of-art algorithms

in Scenario 3.1. The obtained best result of the proposed algorithm in Scenario 3.2 is 6.63% lesser than SOS.

The comparison of the best result of A-CSOS with SOS and the other state-of-the-art algorithms for Scenario 4 is given in Table 7. Table 7 shows that for Scenario 4.1 and Scenario 4.2, the A-CSOS algorithm provides 34.74% and 40.52% better TVD values than SOS. Compared with the most recent ORPD studies in the literature, the result obtained with A-CSOS is also 5.55% better than NGBWCA [15] that the best result of above-mentioned algorithms for Scenario 4.

The control variable settings of best results for Scenario 4 are demonstrated in Table 8. Figures 6 and 7 show that the related dependent variables are within the boundaries after Scenario 3 and Scenario 4 optimizations.

It is observed that Scenario 3.2 and Scenario 4.2 analyses defined as discrete variables are more difficult than the algorithms defined as the continuous variables. Nevertheless, it has been proven that the performance of A-CSOS algorithm in discrete variable ORPD problem is superior to SOS and other algorithms.

Objective function values obtained from the proposed method and SOS over 100 iterations for Scenario 3 and 4 are presented in Figs. 8 and 9. It is appeared from these figures that the SOS algorithm is trapped into local optimum points in the early stage, while the A-CSOS algorithm finds faster

and better values due to increase global and local search capability for both scenarios.

5.3 Test System 3: IEEE 300-bus power system

To evaluate the performance of the proposed algorithm in more complex test systems, the A-CSOS algorithm is implemented on IEEE 300-bus power system as Test System 3. The IEEE 300-bus power system has 145 control variables including sixty-nine continuous variables related to PV bus voltage magnitudes, sixty-two discrete variables related to tunable tap ratios of tap changing transformers with 0.01 p.u. stepwise, forty-five fixed tap transformer, and fourteen discrete variables related to shunt VAR compensators with 1 Mvar stepwise.

Test system data and initial values of the control variables are adapted from [33]. The permissible maximum and minimum bus voltages are 1.1 p.u. and 0.9 p.u., respectively. The maximum and minimum tap ratios of transformers are the same as the bus voltage limits and are 1.1 and 0.9 p.u.

The A-CSOS and SOS algorithm are applied to IEEE 300-bus test system for minimization of P_{loss} as Scenario 5 and minimization of TVD as Scenario 6. The active power loss was 408.3155 MW for initial case, and the reactive power outputs of some generators (e.g., Gen-3, -23, -40, -56) and voltage magnitudes of some buses (e.g., Bus-17, -96, -97, -128, -149) exceeded the related limit values.

Table 9 presents the best values obtained after applying the A-CSOS and SOS algorithm on Test System 3 within the scope of Scenario 5 and Scenario 6 analyses.

Moreover, analogizing the best result of A-CSOS with ALO [22], differential evolutionary PSO (DEEPSO) [34] and mean–variance mapping optimization (MVMO) [34] algorithms is given in Table 9. It should be noted that the DEEPSO and MVMO algorithms were the two best algorithms in the Competition on Application of Modern Heuristic Optimization Algorithms for Solving Optimal Power Flow Problems held in 2014 [34].

According to results, P_{loss} is decreased to a minimum value of 367.1255 MW from the initial P_{loss} of 408.3155 MW via A-CSOS, which is the best value in reported results. The tap settings of transformers and Mvar output of shunt VAR compensators for the best result of A-CSOS and SOS algorithms are demonstrated in Figs. 10 and 11, respectively.

After Scenario 6 optimization, where TVD minimization is performed, the TVD value of 5.4286 p.u. initially decreased to 2.7113 p.u. The tap ratios of transformers and the output of shunt compensators for the best result in Scenario 6 are demonstrated in Figs. 12 and 13, respectively.

The dependent variable characteristics after P_{loss} and TVD optimization are demonstrated in Fig. 14. It can be seen that both objective functions are minimized as well as

Table 5 Comparison of the results for Scenario 3

Algorithms	Min P_{loss} , MW	Mean P_{loss} , MW	Std.
HFA [17]	134.2400	134.8499	0.008814
GWO ^a [18]	131.2620	NR ^b	NR ^b
BBO [8]	128.9700	NR ^b	NR ^b
PSO-ICA [13]	127.8247	NR ^b	NR ^b
GSA [10]	127.7603	NR ^b	NR ^b
OGSA [11]	126.9900	127.1400	0.000088
EMA [24]	126.2200	127.0111	0.000872
SOA ^a [9]	126.0272	130.0486	0.032134
CPVEIHBMO [21]	124.0983	NR ^b	NR ^b
PSOGSA [15]	122.4709	NR ^b	NR ^b
ALC-PSO [12]	121.5300	123.1400	0.000091
NGBWCA [20]	121.4700	NR ^b	NR ^b
GWO [18]	120.6500	NR ^b	NR ^b
ABC ^a [22]	120.4288	NR ^b	NR ^b
ALO ^a [22]	119.7792	NR ^b	NR ^b
SOS ^a	127.7347	132.3327	3.36735
A-CSOS ^a	119.4842	124.4001	2.021968
SOS	123.9277	132.1256	3.82281
A-CSOS	118.4089	123.0515	1.803449

^aDiscrete variable is considered in this result

^bNot reported

Table 6 Optimal value of control variables for best result of P_{loss} optimization on Test System 2

Variable	Scenario 3.1		Scenario 3.2		Variable	Scenario 3.1		Scenario 3.2	
	A-CSOS	SOS	A-CSOS	SOS		A-CSOS	SOS	A-CSOS	SOS
V_{G1} (p.u.)	0.9681	0.9802	0.99045	0.96151	V_{G89} (p.u.)	1.0600	1.0230	1.05506	1.04448
V_{G4} (p.u.)	1.0077	1.0088	1.02209	1.00003	V_{G90} (p.u.)	1.0436	1.0124	1.03021	1.02911
V_{G6} (p.u.)	0.9977	1.0072	1.01467	0.98367	V_{G91} (p.u.)	1.0475	1.0315	1.03437	1.03254
V_{G8} (p.u.)	1.0395	1.0476	1.01884	1.01613	V_{G92} (p.u.)	1.0414	1.0055	1.03505	1.03169
V_{G10} (p.u.)	1.0577	1.0495	1.05989	1.05961	V_{G99} (p.u.)	1.0336	0.9975	1.03202	0.99976
V_{G12} (p.u.)	0.9886	1.0049	1.01139	0.98190	V_{G100} (p.u.)	1.0352	1.0002	1.03045	1.04159
V_{G15} (p.u.)	0.9952	1.0036	1.00918	0.98653	V_{G103} (p.u.)	1.0211	0.9862	1.00855	1.03034
V_{G18} (p.u.)	0.9987	1.0066	1.01316	0.98489	V_{G104} (p.u.)	1.0029	0.9727	1.00558	1.02255
V_{G19} (p.u.)	0.9967	1.0029	1.00784	0.98439	V_{G105} (p.u.)	0.9968	0.9706	1.00401	1.02084
V_{G24} (p.u.)	1.0367	1.0428	1.02385	1.00871	V_{G107} (p.u.)	0.9834	0.9728	1.01079	1.03200
V_{G25} (p.u.)	1.0596	1.0600	1.04821	1.04122	V_{G110} (p.u.)	1.0078	0.9578	0.98743	1.00062
V_{G26} (p.u.)	1.0599	1.0600	1.05999	0.99239	V_{G111} (p.u.)	1.0250	0.9671	0.99619	0.98757
V_{G27} (p.u.)	1.0225	1.0240	1.01281	0.99010	V_{G112} (p.u.)	0.9977	0.9418	0.97287	1.01774
V_{G31} (p.u.)	1.0104	1.0198	1.00088	0.97732	V_{G113} (p.u.)	1.0121	1.0289	1.02056	1.00629
V_{G32} (p.u.)	1.0173	1.0265	1.00500	0.98996	V_{G116} (p.u.)	1.0600	1.0576	1.05994	0.99797
V_{G34} (p.u.)	1.0357	1.0049	1.01394	1.01611	T_8 (p.u.)	1.0194	1.0373	0.97000	1.00000
V_{G36} (p.u.)	1.0339	1.0001	1.00676	1.01310	T_{32} (p.u.)	1.0444	0.9903	1.06000	0.99000
V_{G40} (p.u.)	1.0163	0.9888	1.00353	1.00597	T_{36} (p.u.)	1.0147	1.0066	1.00000	0.99000
V_{G42} (p.u.)	1.0211	0.9941	1.00618	1.00926	T_{51} (p.u.)	0.9866	1.0276	1.01000	0.97000
V_{G46} (p.u.)	1.0315	1.0103	1.03318	1.00570	T_{93} (p.u.)	0.9996	0.9668	0.99000	0.96000
V_{G49} (p.u.)	1.0439	1.0247	1.04477	1.02096	T_{95} (p.u.)	1.0139	1.0999	1.01000	0.99000
V_{G54} (p.u.)	1.0051	0.9931	1.01528	0.99911	T_{102} (p.u.)	0.9811	0.9943	0.98000	1.04000
V_{G55} (p.u.)	1.0041	0.9869	1.01577	0.99650	T_{107} (p.u.)	0.9559	0.9715	0.97000	0.94000
V_{G56} (p.u.)	1.0042	0.9901	1.01548	0.99732	T_{127} (p.u.)	0.9980	1.0267	1.00000	0.95000
V_{G59} (p.u.)	1.0363	1.0134	1.04859	1.04221	Q_{C5} (Mvar)	-25.7306	-9.7831	-25.950	-20.7300
V_{G61} (p.u.)	1.0490	1.0048	1.04888	1.03406	Q_{C34} (Mvar)	11.5546	4.3279	5.47000	4.39000
V_{G62} (p.u.)	1.0469	1.0043	1.04620	1.02111	Q_{C37} (Mvar)	-1.5991	-11.8037	-8.4200	-2.5500
V_{G65} (p.u.)	1.0600	1.0561	1.05999	1.01986	Q_{C44} (Mvar)	9.9506	9.1265	9.60000	5.30000
V_{G66} (p.u.)	1.0599	1.0376	1.05995	1.00315	Q_{C45} (Mvar)	5.7313	0.1188	9.04000	1.61000
V_{G69} (p.u.)	1.0595	1.0337	1.05752	1.00915	Q_{C46} (Mvar)	2.5233	0.2667	4.56000	8.35000
V_{G70} (p.u.)	1.0275	1.0152	1.00956	0.98991	Q_{C48} (Mvar)	8.1370	10.0302	8.49000	9.53000
V_{G72} (p.u.)	1.0319	1.0333	1.01245	0.98698	Q_{C74} (Mvar)	11.6349	6.0659	4.84000	7.47000
V_{G73} (p.u.)	1.0282	1.0355	1.01009	1.00089	Q_{C79} (Mvar)	18.1306	7.1566	19.9000	7.45000
V_{G74} (p.u.)	1.0047	0.9751	0.98960	0.96573	Q_{C82} (Mvar)	14.0703	19.2284	15.6400	10.1600
V_{G76} (p.u.)	0.9877	0.9603	0.97983	0.95836	Q_{C83} (Mvar)	8.5930	5.6014	6.83000	9.83000
V_{G77} (p.u.)	1.0261	0.9995	1.02438	1.01497	Q_{C105} (Mvar)	13.8597	17.9772	15.3400	11.2300
V_{G80} (p.u.)	1.0415	1.0153	1.04151	1.04277	Q_{C107} (Mvar)	5.9824	0.1600	2.38000	5.09000
V_{G85} (p.u.)	1.0350	0.9999	1.01564	1.03080	Q_{C110} (Mvar)	1.7745	2.0031	1.70000	3.31000
V_{G87} (p.u.)	1.0323	1.0021	1.00044	1.05979	P_{loss} (MW)	118.4089	123.9277	119.4842	127.7347
					CPU time (s)	692.0560	690.1967	750.3851	703.6804

the related numerous dependent variables are all within the permissible limit values after optimization.

The convergence profile of A-CSOS algorithm for Scenario 5 and Scenario 6 is given in Figs. 15 and 16, respectively.

When the convergence characteristics of the two algorithms are examined, it is clear that the effect of the

features added to the SOS algorithm is more apparent in large power systems and the convergence performance of the A-CSOS algorithm is much better than the SOS algorithm.

Table 7 Comparison of the results for Scenario 4

Algorithms	Min TVD, pu	Mean TVD, pu	Std.
PSOGSA [15]	0.7308	NR ^b	NR ^b
BBO [8]	0.5020	NR ^b	NR ^b
WCA [20]	0.3752	NR ^b	NR ^b
OGSA [11]	0.3666	NR ^b	NR ^b
ALC-PSO [12]	0.3262	0.3281	0.0001
NGBWCA [20]	0.3194	NR ^b	NR ^b
SOS ^a	0.55816	0.812842	0.1769
A-CSOS ^a	0.33198	0.451382	0.06959
SOS	0.46218	0.843000	1.316848
A-CSOS	0.30454	0.414846	0.043144

6 Conclusion

In this paper, a new chaos and global competitive ranking-based symbiotic organisms search (A-CSOS) algorithm is suggested to deal with ORPD that is one of the highly nonlinear and non-convex optimization problem. The most important property of SOS algorithm is not to need any particular algorithmic parameters. SOS algorithm is hybridized with chaos theory and self-adaptive penalty approach for designing A-CSOS.

As has been explained broadly in previous chapters, although chaos was integrated to SOS algorithm in literature, only the local search capability was slightly increased, but global search capability of the SOS was impaired. On the other hand, SOS was tended to trap into local minimum points for the reason that the chaos was only applied to the best organism and the parasitism phase was removed. These problems seem to be more apparent especially in complex, nonlinear and non-convex optimization problems such as ORPD.

The effectiveness and efficiency of the proposed A-CSOS algorithm is demonstrated on IEEE 57-, 118-, and 300-bus test power systems for minimizing P_{loss} and TVD. Simulation results reveal that A-CSOS is provided up to 7.67% P_{loss} improvement and 44.06% TVD improvement considering the SOS. Moreover, it is clear that the proposed A-CSOS yields up to 1.85% better P_{loss} value and 15.32% better TVD value than the best result of reported algorithms to the related test cases. According to statistical data of the results given in each scenarios, A-CSOS is considerably better than SOS, statistically. As the problem gets more complicated, the superiority of the A-CSOS over SOS becomes more apparent. Therefore, the performance of A-CSOS is considerably better than basic SOS. Any reduction of power loss is not only providing energy efficiency but also saving considerable money.

The results proved that global search capability and convergence speed of SOS have been considerably improved by utilizing chaos and self-adaptive penalty strategies. While the chaos helps the optimizer to find near global minimum solution in a very short time, GCR eliminates the trial and error process needed to find the ideal penalty coefficients and helps the optimizer to direct the organisms to the optimal feasible region.

Therefore, A-CSOS is an excellent candidate to be implemented on ORPD and other constrained nonlinear optimization problems for the future researches. Further investigation on the performance of A-CSOS using other chaotic maps and adaptive penalty techniques may prove fruitful. Proposed method can be hybridized with other optimization algorithms for improving or investigating performance of the hybrid algorithms.

Table 8 Optimal value of control variables for best result of TVD optimization on Test System 2

Variable	Scenario 4.1		Scenario 4.2		Variable	Scenario 4.1		Scenario 4.2	
	A-CSOS	SOS	A-CSOS	SOS		A-CSOS	SOS	A-CSOS	SOS
V_{G1} (p.u.)	0.98743	0.9901	0.98675	0.98989	V_{G89} (p.u.)	1.01699	1.0453	1.01446	0.99754
V_{G4} (p.u.)	1.01636	1.0351	1.00846	1.05198	V_{G90} (p.u.)	1.03626	0.9849	0.95651	1.06000
V_{G6} (p.u.)	1.00062	1.0193	1.00069	1.02708	V_{G91} (p.u.)	1.04276	1.0477	0.99226	1.01589
V_{G8} (p.u.)	0.97677	1.0154	0.97836	0.99467	V_{G92} (p.u.)	1.01092	1.0291	1.00559	0.99969
V_{G10} (p.u.)	1.00616	0.9778	1.00449	1.00483	V_{G99} (p.u.)	0.96225	0.9682	1.05480	1.00447
V_{G12} (p.u.)	1.01188	1.0163	1.01224	1.01392	V_{G100} (p.u.)	1.02538	1.0236	1.04179	1.03302
V_{G15} (p.u.)	0.98968	1.0018	1.00332	0.99379	V_{G103} (p.u.)	1.01898	1.0025	1.03094	1.01604
V_{G18} (p.u.)	0.98754	1.0100	1.00845	0.98942	V_{G104} (p.u.)	1.00174	0.9935	1.01592	1.00944
V_{G19} (p.u.)	0.98736	1.0031	1.00299	0.99087	V_{G105} (p.u.)	1.00401	0.9940	1.01115	1.00740
V_{G24} (p.u.)	1.05289	1.0600	1.06000	1.03809	V_{G107} (p.u.)	1.01534	1.0233	0.99912	1.00829
V_{G25} (p.u.)	1.03312	0.9880	0.98354	1.01461	V_{G110} (p.u.)	0.99854	1.0026	0.98883	1.01119
V_{G26} (p.u.)	1.00259	0.9402	0.96235	0.99523	V_{G111} (p.u.)	1.00768	1.0299	0.95795	0.99239
V_{G27} (p.u.)	1.00905	1.0103	1.00430	0.99936	V_{G112} (p.u.)	0.98411	0.9987	1.01886	1.05014
V_{G31} (p.u.)	1.00298	1.0025	1.00452	1.00430	V_{G113} (p.u.)	1.00047	1.0197	1.02539	0.99224
V_{G32} (p.u.)	1.00132	1.0001	1.00594	1.00358	V_{G116} (p.u.)	0.98645	0.9784	0.99010	0.99370
V_{G34} (p.u.)	0.99623	1.0115	1.01325	1.01080	T_8 (p.u.)	0.95774	1.0746	0.94000	1.01000
V_{G36} (p.u.)	0.99194	1.0052	1.00886	1.00943	T_{32} (p.u.)	1.02734	1.0349	1.07000	0.98000
V_{G40} (p.u.)	1.01771	1.0289	1.00204	1.01697	T_{36} (p.u.)	1.00176	0.9799	1.00000	0.99000
V_{G42} (p.u.)	0.97694	0.9418	1.01993	0.97842	T_{51} (p.u.)	0.98510	0.9745	0.97000	0.97000
V_{G46} (p.u.)	1.04331	1.0519	1.03404	1.04466	T_{93} (p.u.)	0.99288	0.9816	0.97000	1.04000
V_{G49} (p.u.)	1.00341	1.0038	1.00387	1.00960	T_{95} (p.u.)	0.97958	0.9977	0.98000	1.00000
V_{G54} (p.u.)	1.02351	1.0229	1.02220	1.02139	T_{102} (p.u.)	1.02732	1.0364	1.03000	1.07000
V_{G55} (p.u.)	1.01369	1.0111	1.01493	1.00456	T_{107} (p.u.)	0.99536	1.0406	0.95000	0.93000
V_{G56} (p.u.)	1.01526	1.0146	1.01564	1.00995	T_{127} (p.u.)	0.96745	1.0323	0.96000	0.94000
V_{G59} (p.u.)	1.01153	1.0108	1.02570	0.96687	Q_{C5} (Mvar)	-0.31042	-9.9388	-26.400	-17.6000
V_{G61} (p.u.)	1.00183	1.0024	1.00189	0.97158	Q_{C34} (Mvar)	7.42403	1.4903	3.34000	8.73000
V_{G62} (p.u.)	0.99718	0.9938	0.99466	0.96103	Q_{C37} (Mvar)	-22.0909	-21.0922	-15.5900	-17.2200
V_{G65} (p.u.)	1.01606	1.0120	1.02338	1.02443	Q_{C44} (Mvar)	9.99495	5.4228	9.99000	4.24000
V_{G66} (p.u.)	1.01461	0.9974	1.01669	0.97804	Q_{C45} (Mvar)	9.99721	3.9528	9.94000	6.02000
V_{G69} (p.u.)	1.05999	1.0526	1.06000	1.05999	Q_{C46} (Mvar)	5.80266	0.0086	7.41000	7.67000
V_{G70} (p.u.)	1.00921	1.0152	1.00351	0.99215	Q_{C48} (Mvar)	4.47224	7.3262	0.01000	8.57000
V_{G72} (p.u.)	0.97148	1.0400	1.05289	0.99500	Q_{C74} (Mvar)	5.70922	11.7285	7.89000	11.7700
V_{G73} (p.u.)	0.99408	1.0309	0.98107	0.97326	Q_{C79} (Mvar)	9.73093	3.8839	4.27000	2.52000
V_{G74} (p.u.)	0.98696	0.9893	0.98392	0.98102	Q_{C82} (Mvar)	19.9995	19.9934	19.3200	9.01000
V_{G76} (p.u.)	0.97191	0.9723	0.96837	0.97514	Q_{C83} (Mvar)	9.95966	9.987	8.50000	8.43000
V_{G77} (p.u.)	1.00959	1.0095	1.00793	1.02184	Q_{C105} (Mvar)	10.2692	13.1059	15.4000	7.08000
V_{G80} (p.u.)	1.01761	1.0199	1.02149	1.04296	Q_{C107} (Mvar)	3.55680	4.6934	3.14000	2.57000
V_{G85} (p.u.)	1.00663	1.0060	1.01056	0.98984	Q_{C110} (Mvar)	5.67025	2.5931	0.43000	0.66000
V_{G87} (p.u.)	1.01444	0.9954	1.05640	1.04214	TVD (p.u.)	0.30454	0.46218	0.33198	0.55816
					CPU time (s)	694.7607	678.5452	716.7083	688.9141

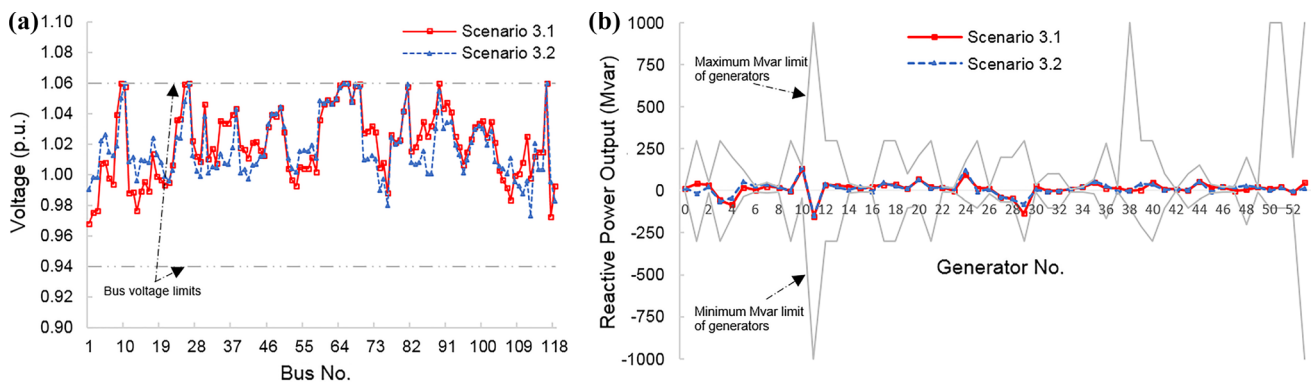


Fig. 6 Dependent variable profiles after Scenario 3 (P_{loss} optimization). **a** Bus voltage profiles. **b** Mvar output of generators

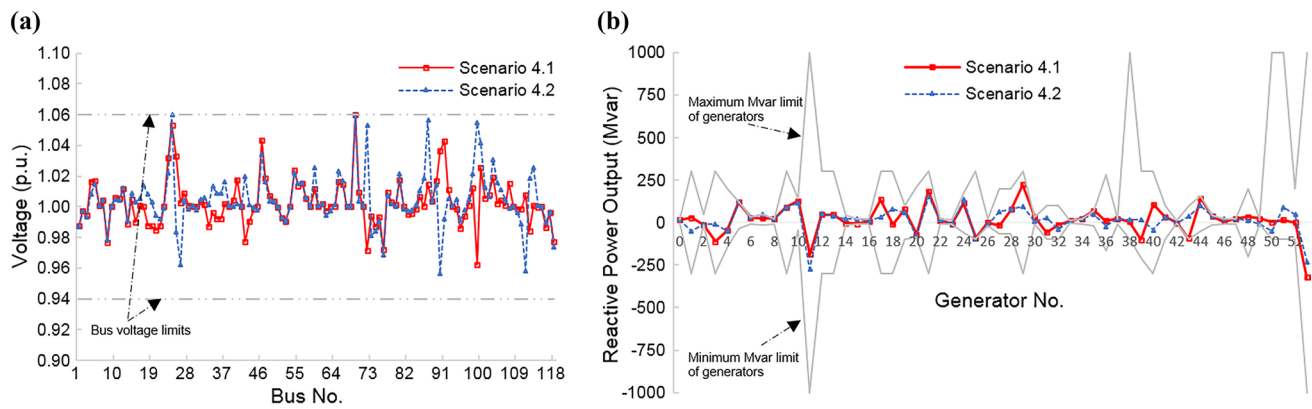


Fig. 7 Dependent variable profiles after Scenario 4 (TVD optimization). **a** Bus voltage profiles. **b** Mvar output of generators

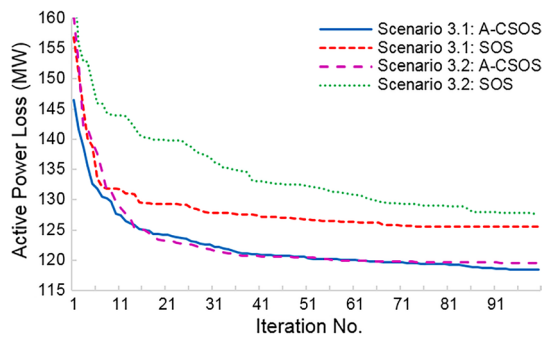


Fig. 8 The convergence profiles of A-CSOS and SOS for Scenario 3

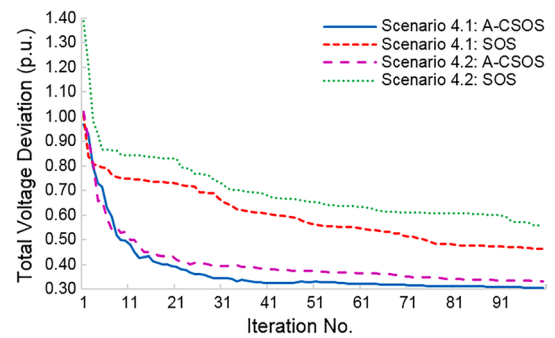


Fig. 9 The convergence profiles of A-CSOS and SOS for Scenario 4

Table 9 Comparison of the results for Scenario 5 and Scenario 6 on Test System 3

Algorithms	Scenario 5: P_{loss} minimization		
	Min P_{loss} , MW	Mean P_{loss} , MW	Std.
Initial	408.3155	–	–
DEEPSO [34]	394.4343	414.6239	42.0360
MVMO [34]	385.6284	394.1294	8.2219
ALO [22]	384.9224	NR ^a	NR ^a
SOS	409.9643	434.7161	11.0400
A-CSOS	367.1255	388.9581	10.0496
	Scenario 6: TVD minimization		
	Min TVD, pu	Mean TVD, pu	Std.
Initial	5.4286	–	–
SOS	4.5420	6.9421	1.0159
A-CSOS	2.7113	4.3876	0.4156

^aNot reported

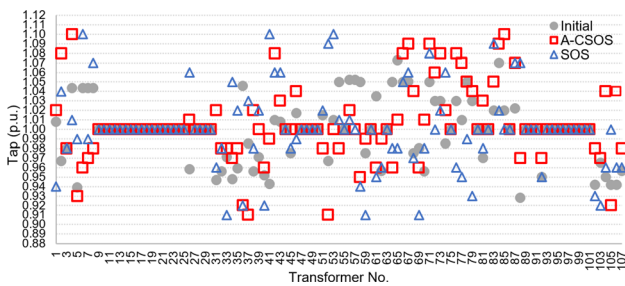


Fig. 10 Tap settings for the best results in Scenario 5

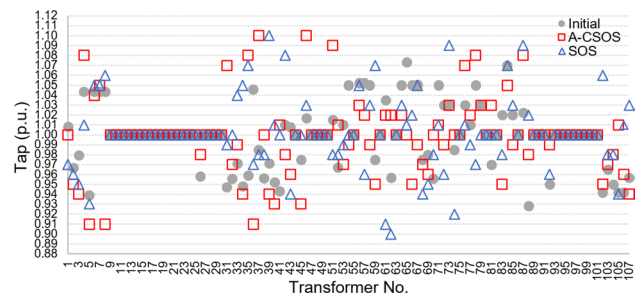


Fig. 12 Tap settings for the best results in Scenario 6

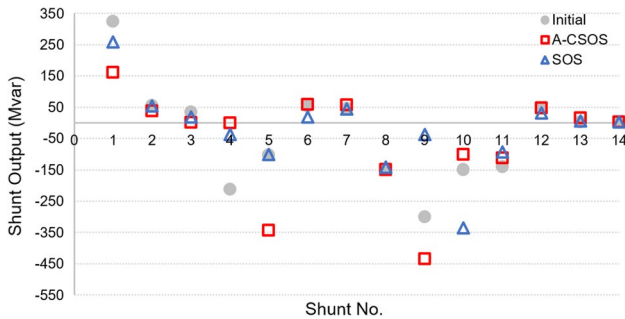


Fig. 11 Shunt compensator settings for the best results in Scenario 5

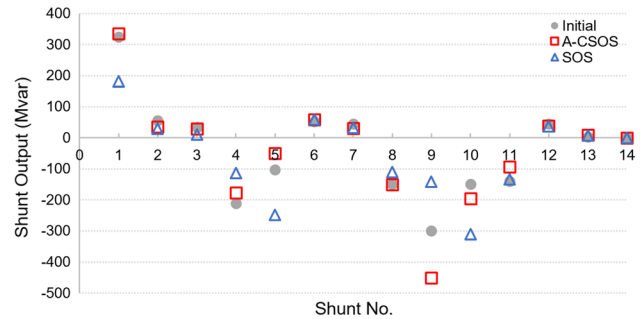


Fig. 13 Shunt compensator settings for the best results in Scenario 6

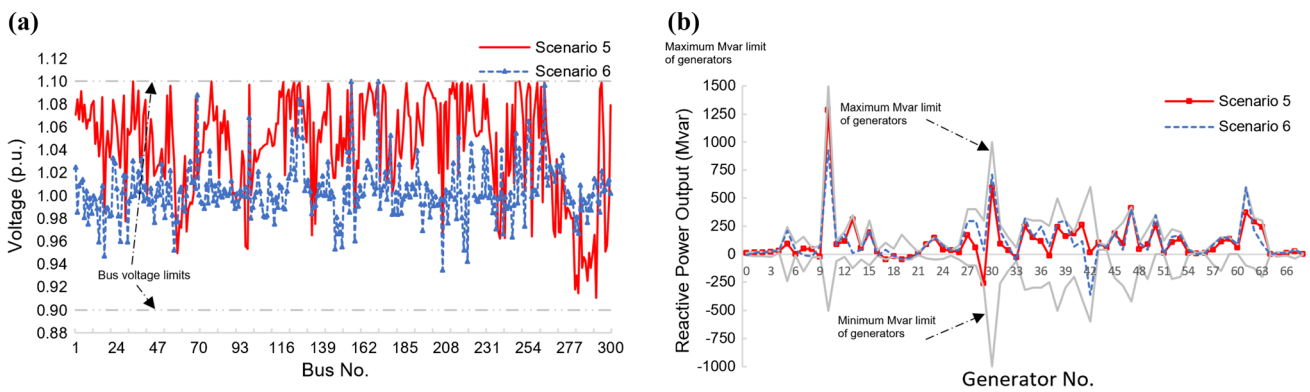


Fig. 14 Dependent variable profiles after P_{loss} and TVD optimization based on A-CSOS algorithm. **a** Bus voltage profiles. **b** Mvar output of generators

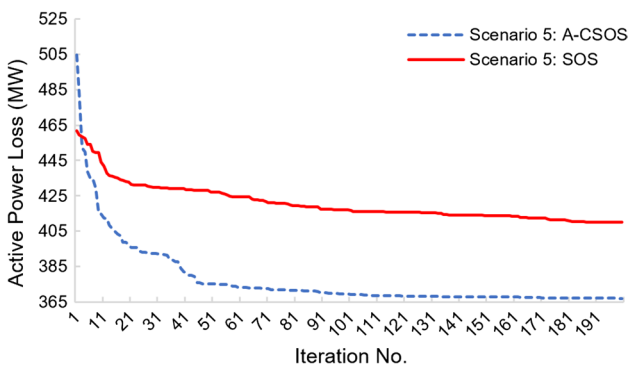


Fig. 15 The convergence profile for Scenario 5

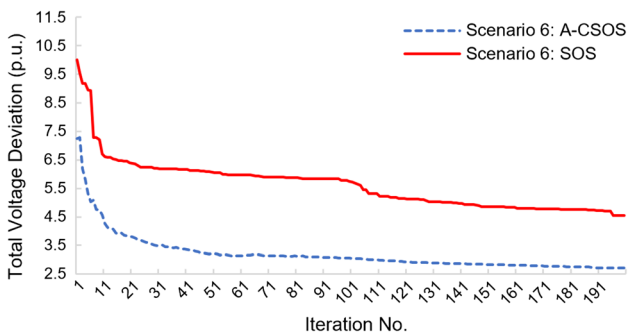


Fig. 16 The convergence profile for Scenario 6

References

1. Terra LDB, Short MJ (1991) Security-constrained reactive power dispatch. *IEEE Trans Power Syst* 6:109–117
2. Lee KY, Park YM, Ortiz JL (1985) A united approach to optimal real and reactive power dispatch. *IEEE Trans Power Appar Syst* 104:1147–1153

3. Quintana VH, Santos-Nieto M (1989) Reactive power dispatch by successive quadratic programming. *IEEE Trans Energy Convers* 4:425–435
4. Granville S (1994) Optimal reactive dispatch through interior point methods. *IEEE Trans Power Syst* 9:136–146
5. Chettih S, Khat M, Chaker A (2011) Voltage control and reactive power optimisation using the meta heuristics method: application in the western Algerian transmission system. *J Artif Intell* 4:12–20
6. Wu QH, Cao YJ, Wen JY (1998) Optimal reactive power dispatch using an adaptive genetic algorithm. *Int J Electr Power Energy Syst* 20:563–569
7. Abou El Ela AA, Abido MA, Spea SR (2011) Differential evolution algorithm for optimal reactive power dispatch. *Electr Power Syst Res* 81:458–464
8. Roy PK, Ghoshal SP, Thakur SS (2012) Optimal VAR control for improvements in voltage profiles and for real power loss minimization using biogeography based optimization. *Int J Electr Power Energy Syst* 43:830–838
9. Dai C, Chen W, Zhu Y, Zhang X (2009) Seeker optimization algorithm for optimal reactive power dispatch. *IEEE Trans Power Syst* 24:1218–1231
10. Duman S, Sonmez Y, Guvenc U, Yorukeren N (2012) Optimal reactive power dispatch using a gravitational search algorithm. *IET Gener Transm Dis* 6:563–576
11. Shaw B, Mukherjee V, Ghoshal SP (2014) Solution of reactive power dispatch of power systems by an opposition-based gravitational search algorithm. *Electr Power Energy Syst* 55:29–40
12. Singh RP, Mukherjee V, Ghoshal SP (2015) Optimal reactive power dispatch by particle swarm optimization with an aging leader and challengers. *Appl Softw Comput* 29:298–309
13. Mehdinejad M, Mohammadi-Ivatloo B, Dadashzadeh-Bonab R, Zare K (2016) Solution of optimal reactive power dispatch of power systems using hybrid particle swarm optimization and imperialist competitive algorithms. *Electr Power Energy Syst* 83:104–116
14. Ghasemi M, Ghavidel S, Ghanbarian MM, Habibi A (2014) A new hybrid algorithm for optimal reactive power dispatch problem with discrete and continuous control variables. *Appl Soft Comput* 22:126–140
15. Radosavljevic J, Jevtic M, Milovanovic M (2016) A solution to the ORPD problem and critical analysis of the results. *Electr Eng*. <https://doi.org/10.1007/s00202-016-0503-1>
16. Chen G, Liu L, Song P, Du Y (2014) Chaotic improved PSO-based multi-objective optimization for minimization of power losses and L index in power systems. *Energy Convers Manag* 86:548–560

17. Rajan A, Malakar T (2015) Optimal reactive power dispatch using hybrid Nelder–Mead simplex based firefly algorithm. *Electr Power Energy Syst* 66:9–24
18. Sulaiman MH, Mustafa Z, Mohamed MR et al (2015) Using the gray wolf optimizer for solving optimal reactive power dispatch problem. *Appl Soft Comput* 32:286–292
19. Mei RNS, Sulaiman MH, Mustafa Z et al (2017) Optimal reactive power dispatch solution by loss minimization using moth-flame optimization technique. *Appl Soft Comput* 59:210–222
20. Heidari AA, Abbaspour RA, Jordehi AR (2017) Gaussian barebones water cycle algorithm for optimal reactive power dispatch in electrical power systems. *Appl Soft Comput* 57:657–671
21. Ghasemi A, Valipour K, Tohidi A (2014) Multi objective optimal reactive power dispatch using a new multi objective strategy. *Int J Electr Power Energy Syst* 57:318–334
22. Mouassa S, Bouktir T, Salhi A (2017) Ant lion optimizer for solving optimal reactive power dispatch problem in power systems. *Eng Sci Technol* 20:885–895
23. Rajan A, Jeevan K, Malakar T (2017) Weighted elitism based ant lion optimizer to solve optimum VAR planning problem. *Appl Soft Comput* 55:352–370
24. Rajan A, Malakar T (2016) Exchange market algorithm based optimum reactive power dispatch. *Appl Soft Comput* 43:320–336
25. Saha S, Mukherjee V (2017) A novel chaos-integrated symbiotic organisms search algorithm for global optimization. *Soft Comput* 22:1–20
26. Cheng MY, Prayogo D (2014) Symbiotic organisms search: a new metaheuristic optimization algorithm. *Comput Struct* 139:98–112
27. Guha D, Roy P, Banerjee S (2017) Quasi-oppositional symbiotic organism search algorithm applied to load frequency control. *Swarm Evol Comput* 33:46–67
28. Secui DC (2017) Large-scale multi-area economic/emission dispatch based on a new symbiotic organisms search algorithm. *Energy Convers Manag* 154:203–223
29. Tejani GG, Savsani VJ, Patel VK (2016) Adaptive symbiotic organisms search (SOS) algorithm for structural design optimization. *J Comput Des Eng* 3:226–249
30. Runarsson T, Yao X (2003) Constrained evolutionary optimization. *Evol Optim Int Ser Oper Res Manag Sci* 48:87–113
31. Munakata T, Sinha S, Ditto WL (2002) Chaos computing: implementation of fundamental logical gates by chaotic elements. *IEEE Trans Circuits Syst I Fundam Theory Appl* 49:1629–1633
32. Runarsson TP, Yao X (2000) Stochastic ranking for constrained evolutionary optimization. *IEEE Trans Evol Comput* 4:284–294
33. Zimmerman RD, Murillo-Sánchez CE, Thomas RJ (2011) MATPOWER: steady-state operations, planning and analysis tools for power systems research and education. *IEEE Trans Power Sys* 26:12–19
34. Erlich I, Lee K, Rueda J, Wildenhues S (2014) Competition on application of modern heuristic optimization algorithms for solving optimal power flow problems. IEEE PES general meeting, Washington, DC, USA. Retrieved from <https://www.uni-due.de/ieee-wgmho/competition2014>. Accessed 4 Oct 2017

Publisher's Note Springer Nature remains neutral with regard to jurisdictional claims in published maps and institutional affiliations.